NANO LETTERS

2007
Vol. 7, No. 3
697−702

Polarity-Dependent Electrochemically Controlled Transport of Water through Carbon Nanotube Membranes

Zuankai Wang,[†,||] Lijie Ci,[‡,||] Li Chen,[§] Saroj Nayak,[§] Pulickel M. Ajayan,*[,‡] and Nikhil Koratkar*[,†]

Department of Mechanical, Aerospace and Nuclear Engineering, Department of Materials Science and Engineering, and Department of Physics, Applied Physics and Astronomy, Rensselaer Polytechnic Institute, Troy, New York 12180

Received December 6, 2006; Revised Manuscript Received January 24, 2007

ABSTRACT

We demonstrate here that water can be efficiently wet and pumped through superhydrophobic aligned multiwalled nanotube membranes by application of a small positive dc bias. At a critical bias (∼1.7 V), with the membrane acting as anode, there is an abrupt transition from a superhydrophobic to hydrophilic state. Interestingly, this phenomenon is strongly polarity dependent; for a negative bias applied to the membrane, 2 orders of magnitude higher bias is required for the transition. The polarity and voltage-dependent wetting that we report could be used to controllably wick fluids through nanotube membranes and could find various applications.

The wettability and capillary transport of water through carbon nanotube membranes have generated much interest[1−7] due to the fundamental biological interest of water flow through nanochannels and for several applications[8−12] in nanofluidic and separation technologies. Aligned carbon nanotube arrays due to their frictionless surfaces[13] and nanoscale pores offer unique possibilities as flow conduits.[14−15] Molecular dynamic simulations[16−17] show that water can flow rapidly through pores created from nanotube assemblies because the process creates ordered hydrogen bonds between the water molecules and the nanotube surfaces. In principle, if water wets the nanotubes, then it can be drawn into the channels of nanotube arrays by capillary suction. However, the top/bottom surfaces made from arrays of vertically aligned nanotubes (nanotube membranes) demonstrate superhydrophobic behavior,[3] inhibiting the wetting of water on these surfaces. For water to wet the nanotube membranes, work has to be done to overcome the energy barrier to effect the transition from the superhydrophobic to hydrophilic state.[18] Although chemical and mechanical means[19−20] can be used to alter the wetting and flow properties of fluids through membranes, an electrical method offers a powerful, nondestructive, and selective way to achieve this. Only very few studies[21−24] have attempted to look at this electrically driven flow through nanochannels; our objective here is to study the mechanics of wetting and electrically driven transport of water through nanotube membranes made of aligned arrays of densely packed multiwalled carbon nanotubes (MWNT). Note that, while in the literature, a nanotube membrane is generally referred to as an aligned nanotube array embedded in a solid matrix (only pathway for mass transport is through the inner pore of the nanotube), in this work, the membrane is an aligned nanotube array with the water transport taking place between the MWNT and not through the interior of the individual tubes.

The MWNT arrays used in this study were grown by thermal chemical vapor deposition of ethylene on Al/Fe catalyst film on Si wafer (Supporting Information). The nanotube membrane yields a nearly spherical droplet (volume ∼2 μL) at the macroscopic level when deionized water is deposited on the surface, as shown in Figure 1. The measured contact angle for the MWNT is ∼163°, indicating that the membrane is superhydrophobic.[25] This measurement is in good agreement with the theoretical calculation based on the well-known Cassie model (Supporting Information). The superhydrophobic MWNT membrane displays a stable character in air, with the contact angle showing no apparent change for up to 15 min. The droplet eventually evaporates on the surface on the membrane without any obvious sinking into the membrane.

We studied the effect of the application of external potential on the droplet stability and wetting behavior. For this, a Pt wire was inserted into the water droplet to establish electrical contact (Figure 1a). First, we studied the droplet

* Corresponding authors. E-mail koratn@rpi.edu (N.K.); ajayan@rpi.edu (P.M.A.). Telephone: 518-276-2630. Fax: 518-276-2623.
[†] Department of Mechanical, Aerospace and Nuclear Engineering.
[‡] Department of Materials Science and Engineering.
[§] Department of Physics, Applied Physics and Astronomy.
[||] These authors contributed equally to this work.

10.1021/nl062853g CCC: $37.00
Published on Web 02/13/2007

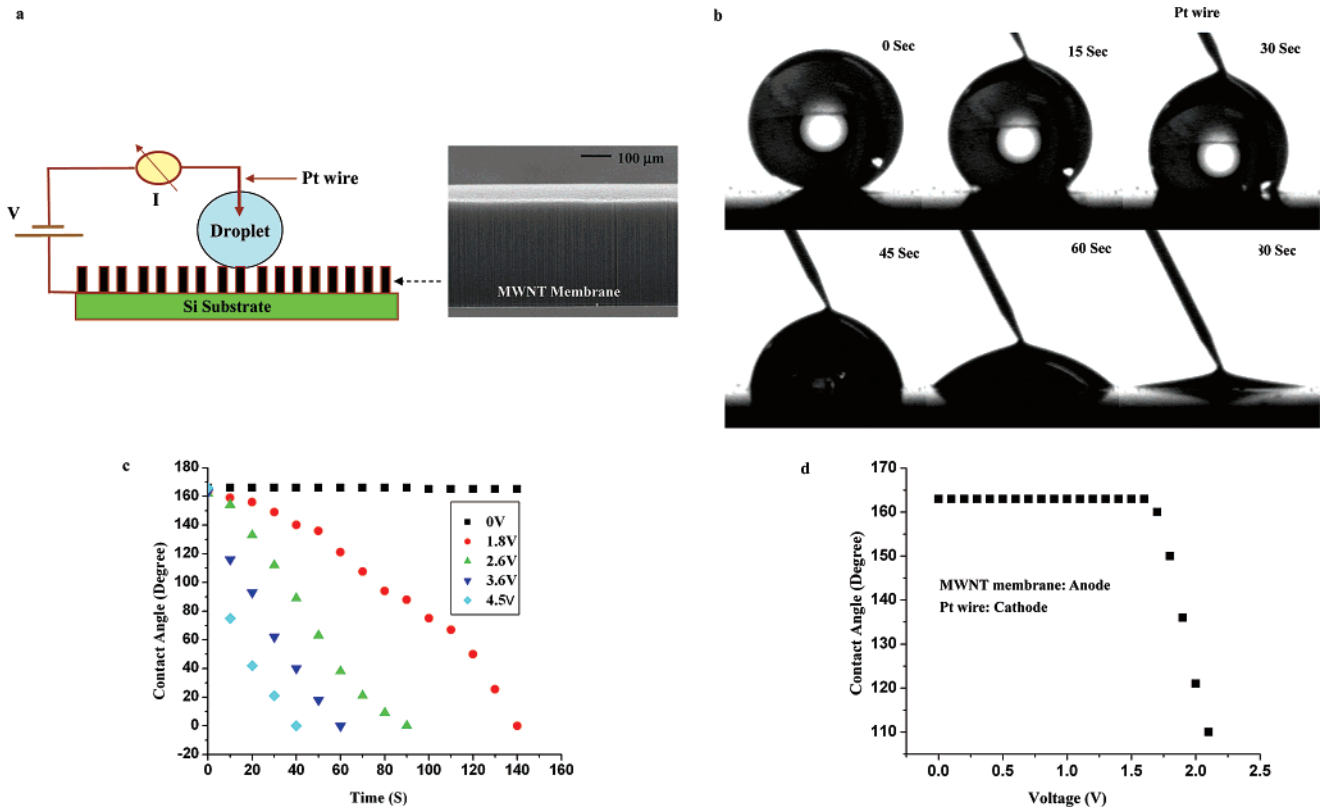

Figure 1. Effect of positive bias (nanotubes as anode) on the droplet response. (a) Left schematic shows the test setup. A deionized water droplet (~2 μL volume) rests on the surface of a superhydrophobic nanotube membrane (right image). A Pt wire probe is inserted into the droplet to establish electrical contact. (b) Snapshots of water droplet shape change with +2.6 V potential applied with multiwalled nanotube film as anode and Pt wire as cathode. The droplet sinks into the nanotube membrane in about 90 s. (c) Apparent contact angle variation with time for different applied voltages. The rate of sinking of the droplet is shown to be dependent on the applied voltage. (d) Apparent contact angle variation with positive potential applied to the MWNT membrane. Below 1.7 V, the contact angle does not change and the droplet does not sink into the membrane. Above 1.7 V, the contact angle changes dynamically due to droplet sinking.

response with the membrane as the anode (positive potential) and the Pt wire as the cathode (negative potential). The droplet shape and contact angle was found to remain unchanged up to a voltage of ~1.7 V. Once this critical voltage was reached, there was an abrupt transition from superhydrophobic state to hydrophilic state, and the droplet rapidly sank into the nanotube forest. This is demonstrated in Figure 1b, which shows snapshots of the droplet sinking into the forest for an applied voltage of 2.6 V. The droplet pumping (or sinking) speed was determined by the applied voltage, as shown in Figure 1c. For an applied voltage of 1.8 V, the droplet took over 140 s to be submerged, while for 2.6 V, the time taken was 90 s. This time was reduced to 60 s for 3.6 V and only 40 s for an applied voltage of 4.5 V. The sinking of the water droplet was not activated unless the applied potential is larger than a threshold value of ~1.7 V, as shown in Figure 1d. Below 1.7 V, the contact angle shows no change with respect to the no-bias case and remains relatively constant at ~163°. Above ~1.7 V, the droplet dynamically sank into the membrane, causing the contact angle to be reduced as shown in the figure. SEM characterization of the nanotube membrane prior to and after wetting confirmed that water is indeed sinking into the membrane and is not merely being electrolyzed on the surface (see Supporting Information).

Next, the droplet sinking dynamics was observed with the membrane as the cathode (negative potential) and the Pt wire as anode; Figure 2a shows snapshots of the droplet shape at different applied voltages. It is interesting to note that the droplet sinking is strongly dependent on the polarity of the membrane electrode. The droplet shape for up to 60 V of applied bias is nearly identical to that at 0 V. For voltages greater than 60 V, a gradual reduction in the contact angle is observed. Figure 2b shows the measured contact angle vs the applied voltage; the threshold voltage needed to activate the sinking of the droplet into the membrane was ~95 V, which is nearly 50-fold greater than when the membrane was the anode. To check whether the Pt wire plays any role in influencing the observed polarity dependence, we also performed a series of control experiments without the Pt wire. For these tests, the water droplet was sandwiched between two identical nanotube membranes. In the first experiment (Figure 3a), the bottom membrane was the anode and the top one was the cathode. The droplet was attracted toward the bottom electrode (anode). In the second experiment (Figure 3b) the top membrane was the anode, while the bottom one was the cathode. Once again the water droplet was pumped toward the anode side. Finally, an ac voltage (Figure 3c) was applied to the two membrane electrodes. The frequency of the ac voltage was varied between 1 Hz

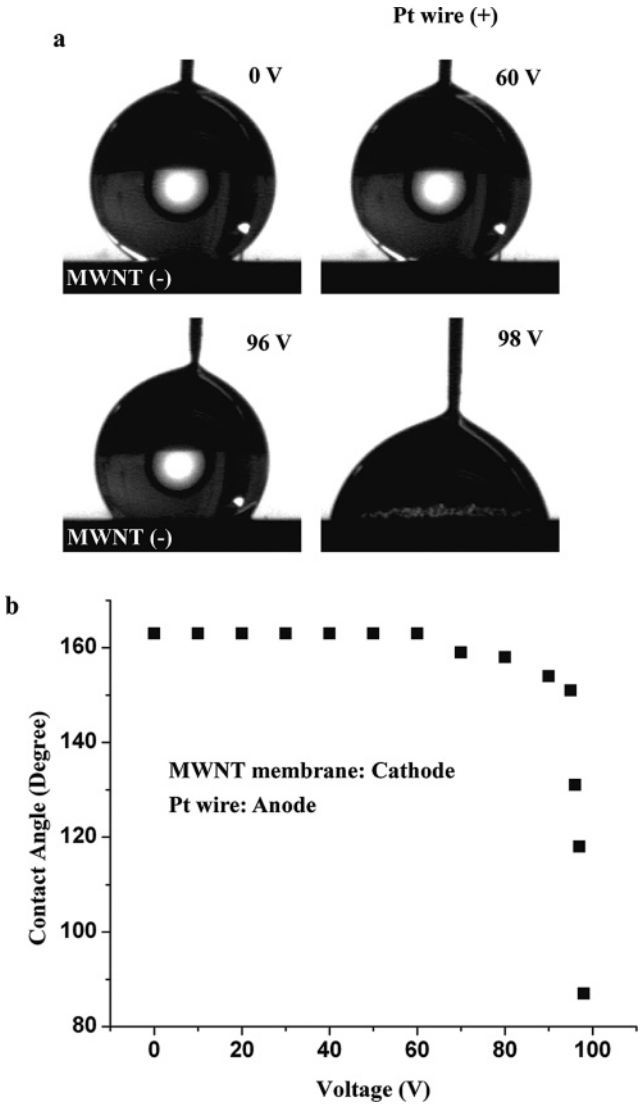

Figure 2. Effect of negative bias (nanotubes as cathode) on the droplet response. (a) Snapshots of water droplet shape change with negative bias applied to the nanotube membrane. The droplet is deionized water. The nanotube membrane is cathode and Pt wire is anode. No significant droplet shape change is observed till ~60 V. (b) Apparent contact angle variation with negative bias applied to the nanotube membrane. The threshold voltage needed to activate the droplet pumping is ~95 V, which is nearly 50-fold greater than that for the positive bias case.

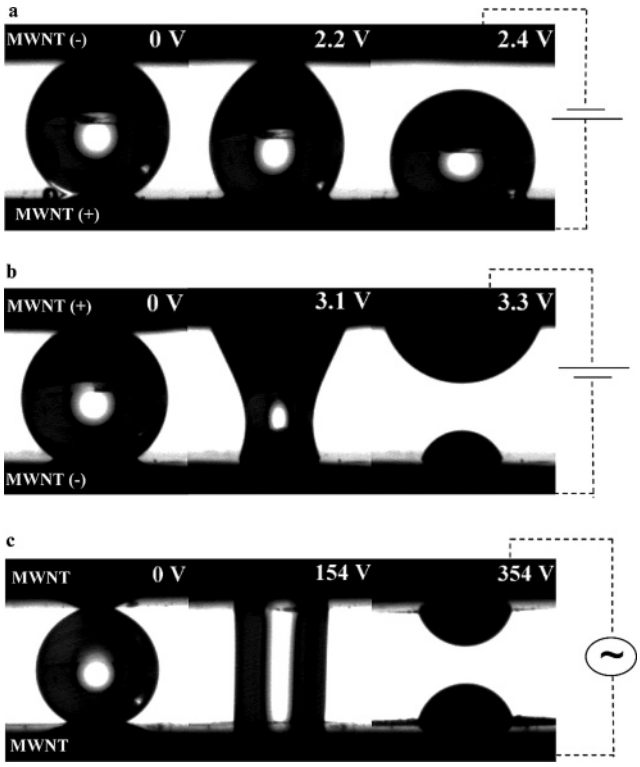

Figure 3. Droplet response with nanotube membrane electrodes as both anode and cathode. (a) The bottom nanotube electrode is the anode; the water droplet is pumped toward the anode side. (b) The top nanotube electrode is the anode; again the droplet is transported toward the anode side (top electrode), indicating the strong polarity dependence of the transport mechanism. (c) An ac voltage (at 5 Hz) is applied across the nanotube electrodes. The water droplet is split symmetrically as shown in the figure. The ac voltage needed to activate the droplet pumping was ~60 Vrms.

and 100 kHz. For the ac bias, we find that the droplet got distributed equally between the top and bottom electrodes. This is expected because each of the membrane electrodes (top and bottom) will alternate as anode and cathode during each cycle of polarity reversal, and no preference was observed toward which side the droplet will be pumped. Figure 3 demonstrates that directional control of the transport wherein the majority of the droplet is either pumped only up or only down or equally in both directions is possible by controlling the polarity of the applied bias.

To explain the above observations, we first considered classical electrowetting phenomenon.[25−26] A recent study has shown that the application of electric potential to a single-walled carbon nanotube attached to an AFM tip can be used to wet mercury.[27] The wetting mechanism is based on repulsion between similar electric charges at the mercury−nanotube interface, which lowers the solid−fluid interfacial tension. However electrowetting is in general weakly dependent on the polarity, as was seen in ref 27. According to the Young−Lippmann equation,[25] the contact angle change with voltage is symmetric for both positive and negative bias. Therefore electrowetting does not appear to explain the abrupt transition from nonwetting to wetting state at low voltages that occurs only when the nanotube membrane is the anode.

To describe the situation we observed, we have considered the role of water electrolysis in the polarity dependence of electrowetting. To examine the extent of electrolysis, we performed current measurements (Figure 4a) between the nanotube membrane electrode and Pt wire using the experimental arrangement of Figure 1. First, a negative bias (−1.0 V) was applied to the membrane for about 15 s; next, the bias was flipped and +1 V was applied. This process of reversing the polarity was repeated at 1.5, 2, and 2.5 V, respectively. Note that the sinking of the droplet (at +2 V bias with the membrane as anode) was accompanied by a sharp increase in the current. However, when the polarity was flipped to −2 V (membrane as cathode), the sinking of the droplet stopped immediately (see snapshot of droplet in Figure 4a) and the steady-state current also decreased. Again,

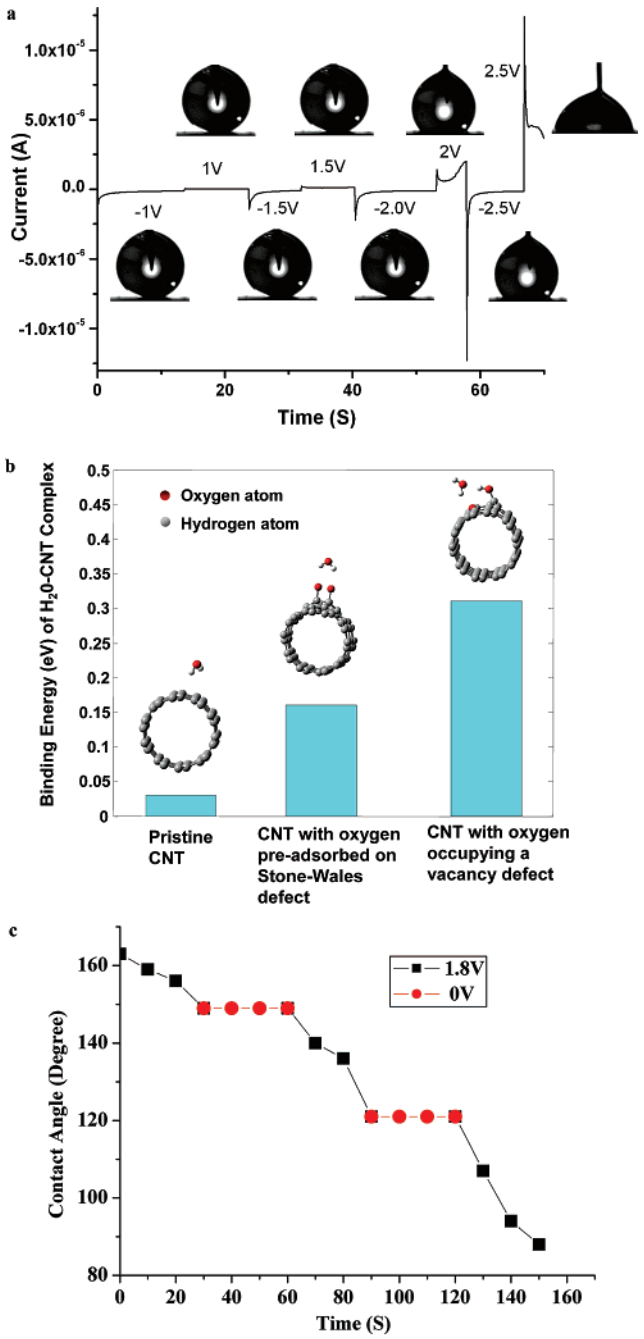

Figure 4. Control experiments and simulations to investigate the polarity dependence of the wetting. (a) Current and droplet shape measurements performed with nanotube membrane and Pt wire as the electrodes. The nanotube film polarity is flipped from the cathode to anode at several voltages (1, 1.5, 2, and 2.5 V). The sinking of the droplet into the positively biased nanotube film (e.g., at +2, +2.5 V potential) is accompanied by a significant increase in the current. Once the polarity is switched, the droplet sinking stops immediately. (b) Binding energy of H_2O molecule with oxidized nanotubes and a pristine (or nonoxidized) nanotube using density functional method. For the oxidized nanotubes, we considered a vacancy defect on the nanotube, which is occupied by oxygen as well as oxygen interacting with a Stone−Wales defect. The insets show the optimized structure after convergence is completed. (c) Selectively stopping and then restarting water transport through the nanotube membrane is demonstrated by simply cycling the applied voltage from 0 to +1.8 V.

when the polarity was switched to +2.5 V, the droplet resumed sinking and the current increased again. The sharp increase in current at +2 and +2.5 V is indicative of electrolysis, which suggests that the sinking of the droplet is linked to the presence of electrolysis in our system. During electrolysis, electrochemical oxidation of the nanotube anode could be responsible for the observed abrupt transition (switching) from nonwetting to wetting state. A recent study[28] has shown that a minimum of 1.7 V of anode voltage is necessary to activate the oxidation of a MWNT electrode, which correlates well to the onset voltage (Figure 1d) for droplet sinking observed in our experiments. To confirm our hypothesis regarding nanotube oxidiation, we performed a simple test; we wetted a nanotube array by application of voltage and then dropped a second droplet on to the nanotube without any voltage being applied. The second droplet also wetted the surface, which is expected because oxidation of the nanotube membrane is an irreversible process. In addition, we observed that the superhydrophobicity of the MWNT membrane was restored by high-temperature treatment in vacuum; this is also expected because oxygen will desorb from the MWNT array at the elevated temperatures.

To understand the effect of attachment of oxygen-containing functional groups on the wetting behavior of the nanotube, we carried out theoretical study (Supporting Information) of interaction of H_2O molecules with a pristine nanotube and an oxidized nanotube using the first-principles density functional method.[29] For the oxidized nanotube, we considered two cases: in the first case, oxygen was preadsorbed on to a Stone−Wales defect, while in the second case, we considered a vacancy defect that is occupied by oxygen (the oxygen molecule dissociates on the vacancy site and one of the atoms is bonded to two dangling carbon atoms, while the other oxygen binds to the third dangling carbon and is saturated with hydrogen). In both cases, we calculated the binding energy of H_2O molecule with the oxidized nanotube and compared the results to the binding of the H_2O molecule with a pristine (or nonoxidized) nanotube. The simulation results are shown in Figure 4b; the insets in the figure show the optimized structure after convergence is completed. Clearly the binding energy of water with the oxidized nanotube (0.16−0.31 eV) is several times that of the pristine nanotube (~0.03 eV) and is comparable to hydrogen-binding energy in liquid water and in water dimmer (~0.19 eV), which confirms that nanotube oxidation indeed makes the membrane strongly hydrophilic. This result also explains why the sinking of the droplet stops when the nanotube polarity is flipped, as shown in Figure 4a. When the nanotube is the cathode, no further oxidation of the nanotube occurs and only the oxidized part is wetted, while the remaining portion of the nanotube is still nonwetting to the water droplet. In this way, the applied bias can be utilized to controllably wet the membrane surface; the transport of water through the nanotube membrane can in fact be repeatedly stopped and then restarted on demand depending on the applied voltage, as demonstrated in Figure 4c. This illustrates a simple low-voltage technique for gating the flow of aqueous liquids in nanofluidic systems.

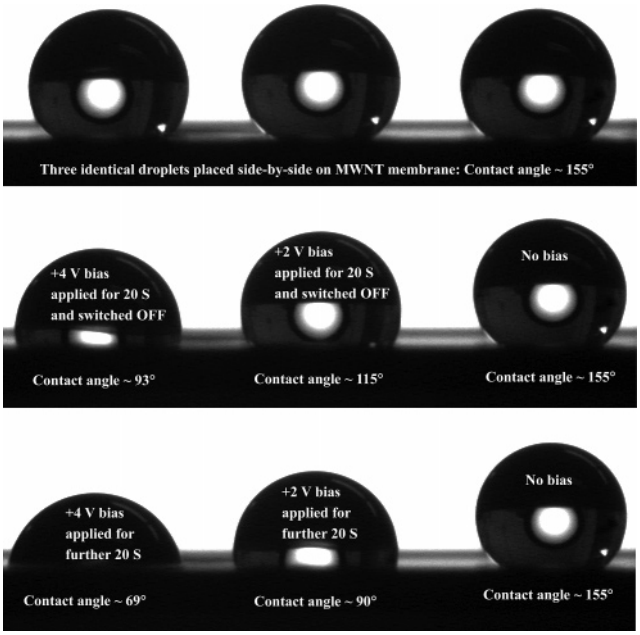

Figure 5. Using electrochemical oxidation of nanotubes to set up a controllable wetting gradient on the membrane surface. Top panel shows three droplets placed side-by-side on the membrane. Middle panel shows that a wetting gradient from 93° to 155° can be set up by biasing the leftmost droplet by +4 V for 20 s and the center droplet by +2 V for 20 s. The lower panel shows that the wetting gradient is increased from 69° to 155° by applying the bias to the leftmost and center droplets for a further 20 s.

Figure 5 illustrates another interesting application of this wetting phenomenon. Three droplets were placed side-by-side on the nanotube surface (see top panel in figure). No voltage was applied to the droplet on the extreme right, and it showed no contact angle change with time. A bias of +2 V was applied to the center droplet for 20 s, and then the bias was switched off. The contact angle of the droplet decreased to 115° in 20 s (middle panel in Figure 5). Next, the bias (+2 V) was applied to the center droplet for a further 20 s. After the bias was switched off, the contact angle of the middle droplet has now decreased to 90°, as shown in the lower panel of Figure 5. The same procedure of biasing the droplet in two 20 s intervals was repeated for the droplet to the extreme left but at a higher potential (+4 V). The contact angle of the droplet decreased to 93° in 20 s and then to 69° in 40 s. Note that, after the voltages were switched off, the sinking of the droplets stopped and the droplets sat stably on the nanotube surface at the reduced contact angles. In this way, it is possible to control precisely the local wettability of any specific point on the nanotube surface, and as shown in Figure 5, a wettability gradient from superhydrophobic to hydrophilic can be engineered on the surface of the nanotube membrane. Such extreme hydrophilic/hydrophobic contrast has a wide range of applications[30] that include biomimetic water-harvesting surfaces, drug release coatings, and microchannel and lab-on-chip devices.

We have also performed control experiments to study the polarity dependence of the electrowetting for liquids other than water (e.g., for mercury). The test results for droplet shape change, and corresponding contact angle measurements are provided in the Supporting Information. For this case, no polarity dependence of the wetting was observed; this is expected because oxidation of the electrode due to electrolysis will not occur for mercury.

In conclusion, we have demonstrated the electrochemically controlled transport of water through nanotube membranes where a critical threshold voltage, which is strongly polarity dependent, is required to activate the water transport. The strong polarity dependence of the wetting suggests that oxygen-containing functional groups are attached as a result of water electrolysis at the nanotube anode, which causes the observed transition from nonwetting to wetting state. The controllable nanofluidic pumping that we demonstrate could have strong applications in biotechnology, lab-on-chip devices, and nanofluidic plumbing systems, which may be designed to controllably move and manipulate the flow of very small volumes of aqueous liquids precisely in space and time.

Acknowledgment. This work is supported by NSF NIRT Award 0403789 to N.K., P.M.A., and S.N. L. C. was supported by the New York State Office of Science, Technology, and Academic Research (Interconnect Focus Center).

Supporting Information Available: Fabrication of nanotube membranes, comparison of MWNT wetting angle with Cassie model, verification that the droplet is sinking into the nanotube membrane, density functional theory calculations, electrowetting experiments with mercury. This material is available free of charge via the Internet at http://pubs.acs.org.

References

(1) Dujardin, E.; Ebbesen, T. W.; Hiura, H.; Tanigaki, K. *Science* **1994**, *265*, 1850−1852.
(2) Barber, A. H.; Cohen, S. R.; Wagner, H. D. *Phys. Rev. Lett.* **2004**, *92*, 186103.
(3) Lau, K. K. S.; Bico, J.; Teo, K. B. K.; Chhowalla, M.; Amaratunga, G. A. J.; Milne, W. I.; McKinley, G. H.; Gleason, K. K. *Nano Lett.* **2003**, *3*, 1701−1705.
(4) Martines, E.; Seunarine, K.; Morgan, H.; Gadegaard, N.; Wilkinson, C. D. W.; Riehle, M. O. *Nano Lett.* **2005**, *5*, 2097−2103.
(5) Kim, B. M.; Qian, S.; Bau, H. H. *Nano Lett.* **2005**, *5*, 873−878.
(6) Majumder, M.; Chopra, N.; Andrews, R.; Hinds, B. R. *Nature* **2005**, *438*, 44−45.
(7) Yum, K.; Yu, M. F. *Phys. Rev. Lett.* **2005**, *95*, 18602.
(8) Jirage, K. B.; Hulteen, J. C.; Martin, C. R. *Science* **1997**, *278*, 655−658.
(9) Daiguji, H.; Yang, P.; Majumdar, A. *Nano Lett.* **2004**, *4*, 137−142.
(10) Karnik, R.; Fan, R.; Yue, M.; Li, D.; Yang, P.; Majumdar, A. *Nano Lett.* **2005**, *5*, 943−948.
(11) Feng, L.; Li, S.; Li, Y.; Li, H.; Zhang, L.; Zhai, J.; Song, Y.; Liu, B.; Jiang, L.; Zhu, D. *Adv. Mater.* **2002**, *14*, 1857−1860.
(12) Prins, M. W. J.; Welters, W. J. J.; Weekamp, J. W. *Science* **2001**, *291*, 277−280.
(13) Cottin-Bizonne, C.; Barrat, J. L.; Bocquet, L.; Charlaix, E. *Nat. Mater.* **2003**, *2*, 237−240.
(14) Holt, J. K.; Gyu Park, H.; Wang, Y.; Stadermann, M.; Artyukhin, A. B.; Grigoropoulos, C. P; Noy, A.; Bakajin, O. *Science* **2006**, *312*, 1034−1037.
(15) Sun, L.; Crooks, R. M. *J. Am. Chem. Soc* **2000**, *122*, 12340−12345.
(16) Hummer, G.; Rasaiah, J. C.; Noworyta, J. P. *Nature* **2001**, *414*, 188−190.
(17) Mann, D. J.; Halls, M. D. *Phys. Rev. Lett.* **2003**, *90*, 195503.
(18) He, B.; Patankar, N. A.; Lee, J. *Langmuir* **2003**, *19*, 4999−5003.
(19) Lafuma, A.; Quere, D. *Nat. Mater.* **2003**, *2*, 457−460.

(20) Zheng, J.; Lennon, E. M.; Tsao, H. K.; Sheng, Y. J.; Jiang, S. *J. Chem. Phys.* **2005**, *117*, 808−818.
(21) Dzubiella, J.; Hansen, J. P. *J. Chem. Phys.* **2005**, *120*, 5001−5004.
(22) Robinson, L.; Hentzell, A.; Robinson, N. D.; Isaksson, J.; Berggren, M. *Lab. Chip* **2006**, *6*, 1277−1278.
(23) Vaitheeswaran, S.; Rassaiah, J.; Hummer, G. *J. Chem. Phys.* **2004**, *121*, 7955−7964.
(24) Vogel, M. J.; Ehrhard, P.; Steen, P. H. *Proc. Natl. Acad. Sci. U.S.A.* **2005**, *102*, 11974−11979.
(25) Krupenkin, T. N.; Taylor, J. A.; Schneider, T. M.; Yang, S. *Langmuir* **2004**, *20*, 3824−3827.
(26) Shapiro, B.; Moon, H.; Garrell, R. L.; Kim, C-J. *J. Appl. Phys.* **2003**, *93*, 5794−5811.
(27) Chen, J. Y.; Kutana, A.; Collier, C. P.; Giapis, K. P. *Science* **2005**, *310*, 1480−1483.
(28) Ito, T.; Sun, L.; Crooks, R. M. *Electrochem. Solid-State Lett.* **2003**, *6*, 4−7.
(29) *Density-Functional Theory of Atoms and Molecules*; Parr, R. G., Yang, W., Eds.; Oxford University Press: Oxford, 1989.
(30) Zhai, L.; Berg, M. C.; Cebeci, F. C.; Kim, Y.; Milwid, J. M.; Rubner, M. F.; Cohen, R. E. *Nano Lett.* **2006**, *6*, 1213−1217.

NL062853G